

Cytosolic RIG-I-like helicases act as negative regulators of sterile inflammation in the CNS

Angela Dann^{1,2,13}, Hendrik Poeck^{3,4,13}, Andrew L Croxford⁵, Stefanie Gaupp¹, Katrin Kierdorf^{1,2}, Markus Knust^{1,2}, Dietmar Pfeifer⁶, Cornelius Maihoefer⁷, Stefan Endres^{3,8}, Ulrich Kalinke⁹, Sven G Meuth¹⁰, Heinz Wiendl¹⁰, Klaus-Peter Knobeloch¹, Shizuo Akira¹¹, Ari Waisman⁵, Gunther Hartmann³ & Marco Prinz^{1,12}

The action of cytosolic RIG-I-like helicases (RLHs) in the CNS during autoimmunity is largely unknown. Using a mouse model of multiple sclerosis, we found that mice lacking the RLH adaptor IPS-1 developed exacerbated disease that was accompanied by markedly higher inflammation, increased axonal damage and elevated demyelination with increased encephalitogenic immune responses. Furthermore, activation of RLH ligands such as 5'-triphosphate RNA oligonucleotides decreased CNS inflammation and improved clinical signs of disease. RLH stimulation repressed the maintenance and expansion of committed T_H1 and T_H17 cells, whereas T-cell differentiation was not altered. Notably, T_H1 and T_H17 suppression required type I interferon receptor engagement on dendritic cells, but not on macrophages or microglia. These results identify RLHs as negative regulators of T_H1 and T_H17 responses in the CNS, demonstrate a protective role of the RLH pathway for brain inflammation, and establish oligonucleotide ligands of RLHs as potential therapeutics for the treatment of multiple sclerosis.

Multiple sclerosis is considered to be an inflammatory demyelinating disease of the CNS. T_H17 cells are involved in the onset and maintenance of experimental autoimmune encephalomyelitis (EAE), the mouse model of multiple sclerosis¹. Mice lacking ROR γ T, IL-17 or IL-23, as well as mice treated with IL-17-blocking antibodies, are less susceptible to EAE than wild-type mice^{2–5}. In fact, IL-17⁺ T cells have been found in CNS lesions of individuals suffering from multiple sclerosis⁶. In addition to IL-17-producing T cells, T_H1 cells might also have a pathogenic effect in multiple sclerosis⁷. Furthermore, EAE can be induced by passive transfer of either T_H1 or T_H17 cells, and the ratio of T_H1 to T_H17 cells of infiltrating lymphocytes determines the tropism of pathology in the CNS^{8,9}.

For efficient priming of myelin oligodendrocyte glycoprotein peptide 35–55 (MOG_{35–55})-specific T_H1 and T_H17 CD4⁺ T cells in secondary lymphoid tissues, an encephalitogenic immune response in the CNS, antigen presenting cells (APCs) such as monocytes and dendritic cells in the periphery or microglia and astrocytes in the CNS are required^{10,11}. Maturation and activation of these APCs is generally mediated through the presence of so-called danger signals^{12,13}. The pattern-recognition receptors implicated in recognition of viral nucleic acids include the membrane bound Toll-like receptors (TLRs) TLR3, TLR7, TLR8 and TLR9 (ref. 14), the RLHs (retinoic

acid-inducible gene I (*RIG-I*), also known as *Ddx58*), melanoma differentiation-associated gene 5 (MDA5, also known as *Ifih1*)¹⁵, the nucleotide-binding oligomerization domain 2 (NOD2)¹⁶, and the recently identified AIM-2 inflammasome¹⁷. RIG-I controls innate immune responses to a wide range of RNA viruses, including influenza virus, Sendai virus and vesicular stomatitis virus, whereas MDA5 controls responses to certain picorna viruses (encephalomyocarditis virus and polio virus)¹⁵. Double-stranded RNA (dsRNA) carrying a 5'-triphosphate (3pRNA) has been identified as the natural ligand for RIG-I and serves as a selective trigger for RIG-I signaling^{18,19}. In contrast, the natural ligand for MDA5 is less well-defined, but there is evidence for the involvement of higher order RNA structures²⁰, and polyinosinic-polycytidylic acid (poly(I:C)), an artificial dsRNA, can elicit MDA5 activation²¹. MDA5 activation by poly(I:C) requires complexation and cytoplasmic delivery (for example, with polyethylenimine (PEI) derivatives)²¹. On receptor engagement by the respective ligands, RIG-I or MDA5 interact with the adaptor protein interferon (IFN)- β promoter stimulator 1 (IPS-1, alternatively MAVS, CARDIF or VISA^{22–25}) to activate downstream signaling cascades that ultimately lead to the production of type-I IFNs and the induction of pro-inflammatory cytokines¹². RLHs are also potential disease modifiers in humans^{26–28}, indicating that RLHs may be involved in

¹Department of Neuropathology, University of Freiburg, Freiburg, Germany. ²Faculty of Biology, University of Freiburg, Freiburg, Germany. ³Institute of Clinical Chemistry and Clinical Pharmacology, University Hospital, University of Bonn, Bonn, Germany. ⁴III. Medizinische Klinik, Klinikum rechts der Isar, Technische Universität München, Munich, Germany. ⁵Institute for Molecular Medicine, University Medical Center of the Johannes Gutenberg University Mainz, Mainz, Germany. ⁶Department of Hematology and Oncology, University Medical Center Freiburg, Freiburg, Germany. ⁷Department of Radiation Oncology, University of Munich, Munich, Germany. ⁸Center of Integrated Protein Science Munich and Division of Clinical Pharmacology, Department of Internal Medicine, University of Munich, Munich, Germany. ⁹Institute for Experimental Infection Research, TWINCORE, Centre for Experimental and Clinical Infection Research, a joint venture between the Helmholtz Centre for Infection Research, Braunschweig and the Hannover Medical School, Hannover, Germany. ¹⁰Department of Neurology, Inflammatory Disorders of the Nervous System and Neuro-oncology, University of Münster, Münster, Germany. ¹¹Department of Host Defense, Research Institute for Microbial Diseases, Osaka University, Japan. ¹²BIOSS Centre for Biological Signaling Studies, University of Freiburg, Freiburg, Germany. ¹³These authors contributed equally to this work. Correspondence should be addressed to M.P. (marco.prinz@uniklinik-freiburg.de).

Received 28 July; accepted 23 September; published online 4 December 2011; doi:10.1038/nn.2964

the regulation of immune homeostasis. Here we analyzed the *in vivo* function of two RLHs, RIG-I and MDA5, and the downstream adaptor protein IPS-1 in the course of sterile inflammation and the induction of encephalitogenic T_H1 and T_H17 cells.

RESULTS

IPS-1 modulates the effector phase of EAE

To investigate the involvement of RLHs in CNS autoimmune diseases, we examined the development of EAE in mice lacking IPS-1, the adaptor for both RIG-I and MDA5. *Ips-1*^{-/-} (also known as *Mavs*) and *Ips-1*^{+/+} mice were immunized with MOG₃₅₋₅₅ emulsified in complete Freund's adjuvant. The mice developed EAE with an incidence of 100% and a similar mean disease onset (Fig. 1a). However, in *Ips-1*^{-/-} mice, the peak of disease was significantly augmented ($P < 0.05$).

Histology performed on *Ips-1*-deficient spinal cords revealed a plethora of infiltrating macrophages (Fig. 1b). The increased influx of macrophages was accompanied by an elevated number of T cells and stronger demyelination as compared with *Ips-1*^{+/+} mice (Fig. 1b–e), whereas there was no statistically significant difference ($P > 0.05$) in axonal damage between *Ips-1*^{-/-} and *Ips-1*^{+/+} mice (Fig. 1f). The number of mature oligodendrocytes was significantly lower ($P < 0.05$) in *Ips-1*^{-/-} mice than in *Ips-1*^{+/+} mice (Fig. 1g).

We next quantified the expression of T_H17 (Fig. 1h), T_H1 (Fig. 1i) and T_H2 factors (Fig. 1j) in the CNS. Notably, all of the T_H17 -related factors were increased in *Ips-1*^{-/-} mice relative to wild-type mice, whereas T_H2 factors remained unchanged, with the exception of GATA3. Similarly, the T_H1 -related factors IL-12p35 and T-bet were elevated in the absence of IPS-1, whereas IFN- γ only showed a general trend toward elevation in *Ips-1*^{-/-} mice. Thus, the more severe EAE in the absence of IPS-1 was linked to a shifted immune response toward T_H1 and T_H17 , with the T_H2 reaction remaining almost normal.

We determined the percentage of $\gamma\delta$ T cells among CD3⁺ T cells, as they have been described as the main producers of IL-17 through the IL-1 β and IL-23 pathway, thereby amplifying T_H17 responses and autoimmunity²⁹ (Supplementary Fig. 1). There was no change in the proportion of $\gamma\delta$ T cells.

Activation of cytosolic helicases dampens CNS autoimmunity

Currently, therapeutic intervention using exogenously administered IFN- β is a primary treatment option for multiple sclerosis^{30–33}. To examine the effect of RLH activation on the course of EAE, we applied 3pRNA (RIG-I ligand) or poly(I:C) (MDA5 ligand) at the peak of disease (Fig. 2a). Activation of RIG-I and MDA5 by 3pRNA or poly(I:C) was achieved using PEI as complexing reagent as described previously²¹. All experimental groups had an incidence of disease of 100%, a similar mean disease onset and peak disease activity. Repeated injections of RNA ligands strongly modified the clinical courses.

Disease severity during the effector phase was markedly diminished in RIG-I- and MDA5-stimulated mice, whereas non-complexed poly(I:C) (TLR3 ligand) or synthetic RNA bearing no 5'-triphosphate (polyA) did not change the disease score (Fig. 2a). Serum levels of IFN- β were measured at different time points after a single dsRNA injection, with the level peaking at 6 h (Fig. 2b).

During the chronic disease phase, many infiltrating macrophages and lymphocytes were present in the spinal cord, and the number of cells present was significantly reduced in MDA5- and RIG-I-stimulated mice ($P < 0.05$; Fig. 2c). Specific myeloid and lymphoid subsets are recruited to the inflamed CNS during EAE^{34–36}. We measured the numbers of CD45^{hi}CD11b⁺ macrophages, Ly-6C^{hi}CD115⁺ 'inflammatory' monocytes, Ly-6C^{lo}CD115⁺ 'resident' monocytes, Ly-6G⁺CD11b⁺ granulocytes, CD4⁺CD3⁺ T_H cells, CD8⁺CD3⁺ T_C cells

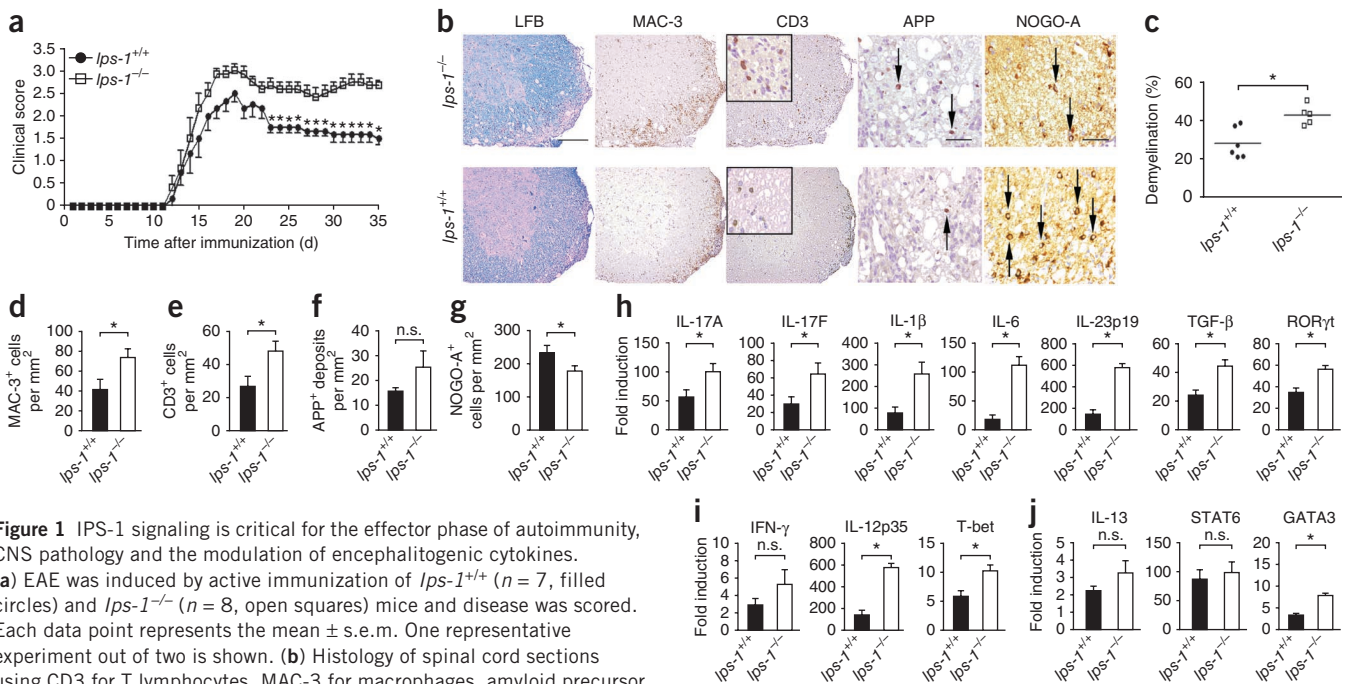
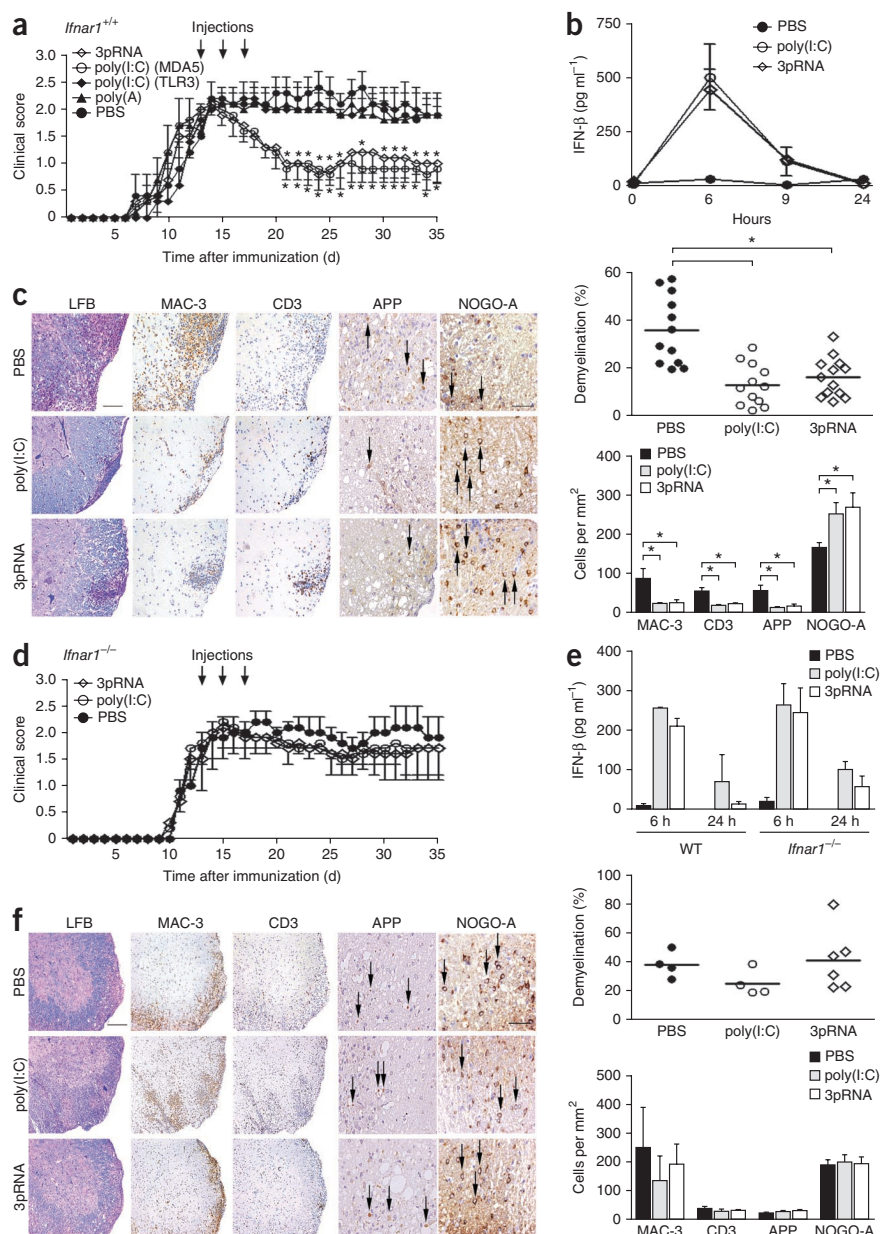


Figure 1 IPS-1 signaling is critical for the effector phase of autoimmunity, CNS pathology and the modulation of encephalitogenic cytokines.

(a) EAE was induced by active immunization of *Ips-1*^{+/+} ($n = 7$, filled circles) and *Ips-1*^{-/-} ($n = 8$, open squares) mice and disease was scored. Each data point represents the mean \pm s.e.m. One representative experiment out of two is shown. (b) Histology of spinal cord sections using CD3 for T lymphocytes, MAC-3 for macrophages, amyloid precursor protein (APP) for axonal damage, luxol fast blue (LFB) for demyelination and NOGO-A for mature oligodendrocytes. Scale bars represent 200 μ m (left) and 50 μ m (right). (c) Quantification of demyelination. Each symbol indicates the mean of one mouse. Data are expressed as mean \pm s.e.m. (d–g) Quantification of MAC-3⁺ cells (d), CD3⁺ cells (e), APP⁺ deposits (f) and NOGO-A⁺ cells (g). n.s., not significant ($P > 0.05$). Data are expressed as mean \pm s.e.m. (h–j) Expression of T_H17 (h), T_H1 (i) and T_H2 -linked (j) factors 19 dpi in the spinal cords of *Ips-1*^{+/+} or *Ips-1*^{-/-} mice. Data are expressed as the ratio of induced factors normalized to endogenous GAPDH compared with healthy controls and expressed as mean \pm s.e.m. At least four animals were used per group. * $P < 0.05$.

Figure 2 Activation of the cytosolic helicases modulates CNS autoimmunity through an IFNAR-dependent pathway. **(a)** EAE was induced by active immunization of *Ifnar1*^{+/+} animals intravenously treated with 25 μ g of complexed 3pRNA ($n = 7$), complexed poly(I:C) (MDA5, $n = 8$), non-complexed poly(I:C) (TLR3, $n = 6$), poly(A) ($n = 5$) or phosphate-buffered saline (PBS, $n = 5$) at 13, 15 and 17 dpi (indicated by arrows). Each data point represents the mean of at least six mice. * $P < 0.05$. One representative experiment out of three is depicted. **(b)** Kinetics of IFN- β serum levels at indicated time points in non-immunized *Ifnar1*^{+/+} mice after the first intravenous injections of PBS (13 dpi), complexed poly(I:C) (MDA5), or complexed 3pRNA. Each data point represents the mean \pm s.e.m. of at least three mice. **(c)** Characterization of infiltrates and demyelination in treated EAE mice on 35 dpi. Histology of CNS sections using LFB for demyelination, MAC-3 for macrophages, CD3 for T lymphocytes, APP for axonal damage and NOGO-A for oligodendrocytes, and quantification thereof (right). Arrows point to APP deposits. Scale bars represent 200 μ m (left) and 50 μ m (right). Each symbol indicates one mouse. Data are expressed as mean \pm s.e.m. **(d)** Clinical scores in *Ifnar1*^{-/-} animals treated intravenously with 25 μ g complexed 3pRNA ($n = 6$), complexed poly(I:C) ($n = 6$) or PBS ($n = 5$) at 13, 15 and 17 dpi (arrows). Data shown are from one representative experiment out of two independent experiments with at least five mice per group. There were no statistically significant differences ($P > 0.05$). Data are expressed as mean \pm s.e.m. **(e)** Unchanged IFN- β serum levels in wild-type or *Ifnar1*^{-/-} mice 6 and 24 h after intravenous application of PBS, complexed poly(I:C) or complexed 3pRNA. **(f)** Histopathology of spinal cords in *Ifnar1*^{-/-} mice on 35 dpi, visualized by LFB for myelin integrity, MAC-3 for invading macrophages, CD3 for T cells, APP for axonal damage and NOGO-A for oligodendrocytes, and quantification thereof (right). Scale bars represent 200 μ m (left) and 50 μ m (right). Arrows point to APP deposits and NOGO-A⁺ cells. Each symbol indicates one mouse. Data are expressed as mean \pm s.e.m. There were no significant differences between the groups ($P > 0.05$).



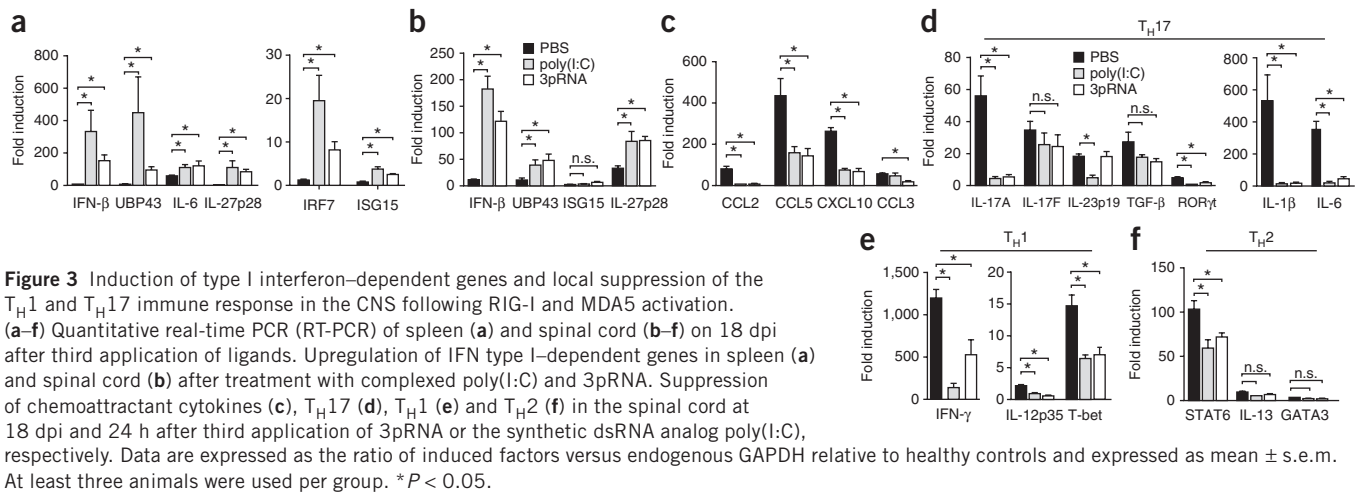
and Foxp3⁺CD3⁺ regulatory T (T_{reg}) cells present in the CNS (Supplementary Fig. 2), and found that all investigated lymphoid and myeloid populations were diminished in the CNS following RLH activation. Furthermore, the myelin damage was decreased in both of the groups treated with RNA ligands (Fig. 2c).

Disease amelioration by RLH requires IFNAR signaling

To examine the role of type 1 IFN receptor (IFNAR) signaling in RIG-I/MDA5-mediated disease suppression, we used IFNAR-deficient mice. In *Ifnar1*^{-/-} mice, the onset of neurological signs of disease was similar to that in control mice, whereas the effector phase was significantly enhanced ($P < 0.05$), as described previously^{30,31}. Moderately diseased *Ifnar1*^{-/-} mice were then repeatedly treated with RLH agonists, and the clinical course of disease was subsequently monitored (Fig. 2d). Unlike wild-type mice (Fig. 2a), *Ifnar1*^{-/-} mice showed no improvement of the clinical course of EAE after treatment with RIG-I or MDA5 ligands. Notably, serum IFN- β levels in

Ifnar1^{-/-} mice were normal (Fig. 2e). Histopathological examination of the CNS revealed a similar pattern of axonal damage, demyelination and mononuclear infiltration (Fig. 2f).

To further determine the effect of RLH activation on local cytokines, we examined spleens (Fig. 3a) and spinal cords (Fig. 3b–f). IFN- β , IRF7, ISG15 and UBP43 were strongly induced compared with controls treated with phosphate-buffered saline (PBS) (Fig. 3a,b). IL-27p28 was also markedly induced in both compartments. MDA5 activation decreased the number of transcripts of the T_H17-related factors IL-1 β , IL-6, IL-23p19, TGF- β , ROR γ T and IL-17A, whereas RIG-I activation reduced the number of IL-1 β , IL-6, TGF- β , ROR γ T and IL-17A transcripts (Fig. 3d). IL-17F levels remained unchanged. The T_H1 factors IFN- γ , T-bet and IL-12p35 (Fig. 3e), as well as the T_H2-related factor STAT6 (Fig. 3f), were diminished compared with the PBS-treated group, whereas IL-13 and GATA3 were not influenced. Chemokines were downregulated after treatment (Fig. 3c).



IFNAR on myeloid subsets mediates RLH effects

We then analyzed IFN- β production by specific peripheral immune cell subsets on RIG-I and MDA5 stimulation. Bone marrow-derived macrophages (BMDMs) responded with robust IFN- β release after selective RIG-I activation and, to a lower extent, MDA5 activation (Fig. 4a). Studies with bone marrow-derived dendritic cells (BMDCs) isolated from mice that were genetically deficient for TLR7 (Fig. 4b), MDA5 or RIG-I (Fig. 4c) indicated that the induction of IFN- β in BMDCs by 3pRNA and poly(I:C) depended on the presence of RIG-I or MDA5, respectively, but not on TLR7. 3pRNA induced IFN- β in BMDCs or plasmacytoid dendritic cells, but not in B, NK or T cells (Fig. 4d). We next studied the induction of innate immune responses by 3pRNA *in vivo*. Intravenous or intraperitoneal injection of 3pRNA induced a systemic increase of IFN- β levels, although intravenous injection was superior in terms of IFN- β induction (Fig. 4e). To visualize the fate of injected RLH ligands *in vivo*, we injected fluorescein isothiocyanate (FITC)-labeled RNA into EAE mice (Supplementary Fig. 3). Flow cytometry revealed that fluorescently labeled RNA mainly reached the spleen and that the labeled cells consisted of mostly CD11b $^+$ CD11c $^+$ dendritic cells, a few CD11b $^+$ CD11c $^-$ macrophages and no CD4 $^+$ T cells. Notably, labeled RNA could not be detected in the diseased spinal cord, indicating that RLH engagement occurred mainly in the periphery.

To test the involvement of distinct myeloid subsets in RLH-mediated and IFNAR-dependent effects, we used *Ifnar1*^{loxP/loxP}; *LysM-cre* mice as described previously³¹. In these mice IFNAR

is absent on CD11b $^+$ Ly-6C^{lo} monocytes, CD11b $^+$ Ly-6C^{hi} monocytes, CD11b $^+$ CD45^{lo} microglia and CD11b $^+$ Gr-1 $^+$ granulocytes, but not on plasmacytoid dendritic cells or myeloid DCs³¹. All of the groups showed a similar disease incidence and disease onset (Fig. 5a). Application of 3pRNA and poly(I:C) significantly decreased ($P < 0.05$) the mean clinical course in *Ifnar1*^{loxP/loxP}; *LysM-cre* mice. Notably, the RLH-associated IFN- β release in the serum was similar in *Ifnar1*^{loxP/loxP} and *Ifnar1*^{loxP/loxP}; *LysM-cre* mice (Fig. 5a). Similarly, CNS damage was clearly reduced (Supplementary Fig. 4). These data indicate that the engagement of IFNAR on monocytes, macrophages, microglia and granulocytes does not account for the suppression of CNS autoimmunity on treatment with dsRNAs.

To determine whether IFNAR engagement on dendritic cells is required for RNA ligand-mediated disease attenuation, we crossed conditional (*loxP* flanked) IFNAR mice with a transgenic line expressing the Cre recombinase under the control of the *Cd11c* (also known as *Ilgax*) promoter. In these mice, IFNAR deletion is restricted to dendritic cells and does not affect receptor expression on CD11b $^+$ macrophages³⁷.

All of the *Ifnar1*^{loxP/loxP}; *Cd11c-cre* mice developed neurological signs of disease, such as tail weakness and paralysis, starting at about 10–12 days post immunization (dpi; Fig. 5b). After RLH activation, the effector phases were similar in all of the treated groups, suggesting that IFNAR expression on dendritic cells is required for RNA ligand-mediated disease suppression. Notably, *Ifnar1*^{loxP/loxP}; *Cd11c-cre* mice were able to produce normal type I IFN responses, as indicated by normal IFN- β serum levels after RLH activation (Supplementary Fig. 5). Examination of the CNS revealed no

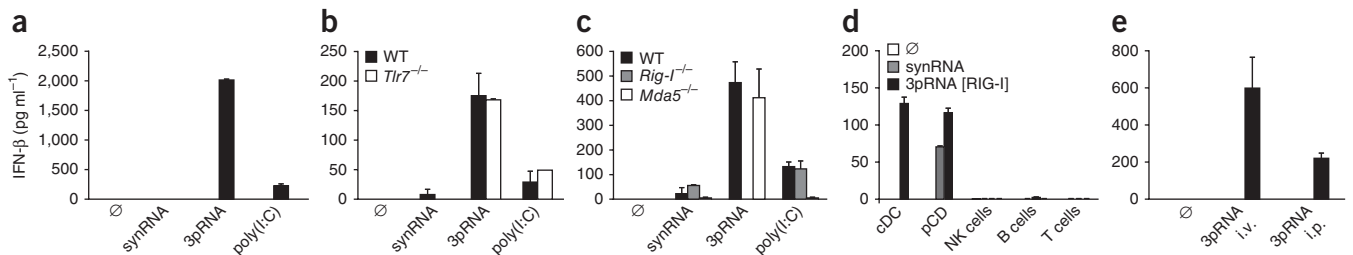
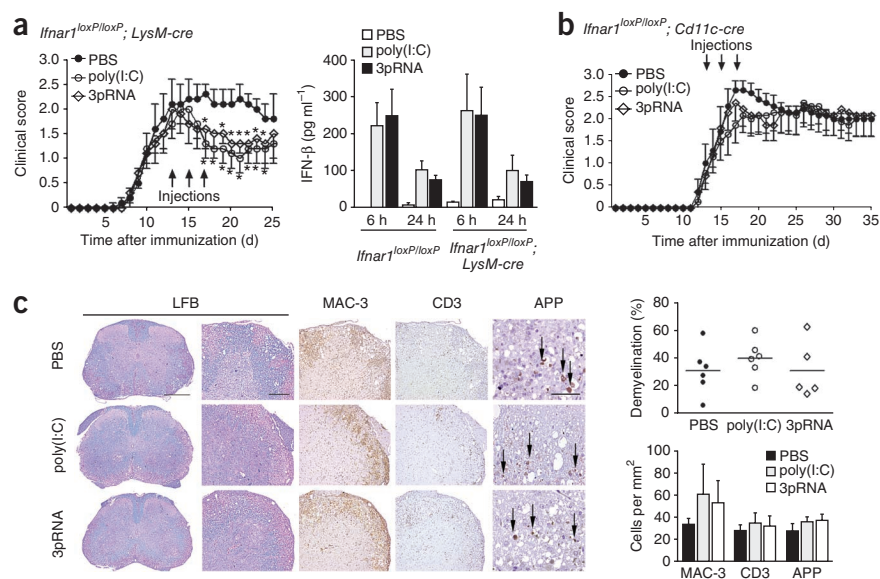


Figure 4 Type I IFN induction by dsRNAs in the hematopoietic compartment is cell-type specific and requires RIG-I and MDA5, but not TLR7. (a–d) IFN- β concentrations in culture supernatants of BMDMs (a), BMDCs of wild-type (WT) and *Tlr7*^{-/-}, *Rig-I*^{-/-} or *Mda5*^{-/-} mice (b,c), and conventional dendritic cells (cDCs), plasmacytoid dendritic cells (pCDs), NK cells, B cells and T cells. (d) were measured by ELISA 24 h after transfection with the indicated RNAs and lipofectamine. Data are shown as means \pm s.e.m. of two independent experiments. synRNA, synthetic RNA. (e) Complexed 3pRNA (25 μ g) was injected into wild-type animals intravenously (i.v.) or intraperitoneally (i.p.) and serum IFN- β levels were measured 6 h later by ELISA. Data depicted are from one representative experiment of at least two independent experiments. Data are expressed as mean \pm s.e.m. \emptyset , nothing added.

Figure 5 IFNAR signaling on dendritic cells rather than on monocytic cells is required for dsRNA-mediated suppression of CNS autoimmunity. **(a)** Left, disease course after RNA injection in the absence of IFNAR on macrophages, monocytes and neutrophils. *Ifnar1^{loxP/loxP}; LysM-cre* mice were treated intravenously with complexed 3pRNA ($n = 6$), complexed poly(I:C) ($n = 7$) or PBS ($n = 5$) at the peak of disease (arrows). Right, serum IFN- β levels over time measured by ELISA.

* $P < 0.05$. The results are representative of two independent experiments. Each data point represents the mean \pm s.e.m. of at least six mice. **(b)** Active EAE in *Ifnar1^{loxP/loxP}; Cd11c-cre* mice treated with PBS, complexed poly(I:C), complexed 3pRNA at the peak of disease (arrows). There were no statistically significant different time points ($P < 0.05$). The results are representative of two independent experiments. Each data point represents the mean \pm s.e.m. of at least five mice.

(c) Histopathological examination of CNS infiltrates and histopathology in *Ifnar1^{loxP/loxP}; Cd11c-cre* mice at 35 dpi treated with immunostimulatory RNAs. Left, the normal pattern of infiltrates and myelin damage in mice devoid of IFNAR on CD11c⁺ cells. Right, quantification of the results on the left. Each symbol indicates one mouse. Data are expressed as mean \pm s.e.m. There were no significant differences ($P < 0.05$). Scale bars represent 500 μ m (left), 200 μ m (middle) and 50 μ m (right).



obvious differences in the pattern of mononuclear cell infiltration (Fig. 5c). Accordingly, myelin and axonal damage were similar in all of the groups that we examined. Overall, these data indicate that dendritic cell-specific IFNAR expression is essential for mediating RLH-mediated effects.

RLH activation inhibits T_{H1} and T_{H17} expansion and survival

We next addressed whether RLH activation interferes with maintenance or expansion of committed T_{H1} or T_{H17} cells. To this end, we exposed lymph node cells containing differentiated T_{H1} and T_{H17} cells from EAE mice at 18 dpi after the third RLH activation to increasing MOG₃₅₋₅₅ concentrations *in vitro* (Fig. 6a). MOG₃₅₋₅₅-stimulated T-cell expansion was significantly lower ($P < 0.05$) in cells derived from RNA ligand-treated wild-type mice compared with the PBS-treated group (Fig. 6a). Notably, 3pRNA- and poly(I:C)-mediated suppression of T-cell expansion was dependent on the presence of IFNAR on dendritic cells (Fig. 6b,c). Similarly, the treatment effect correlated with a reduction in the IL-17 and IFN- γ production in MOG₃₅₋₅₅-stimulated T cells from wild-type mice, but not from *Ifnar1^{-/-}* or *Ifnar1^{loxP/loxP}; Cd11c-cre* mice (Fig. 6a-c).

We further investigated the mechanisms underlying the role of RNA ligands as survival signals that allow committed T_{H1} and T_{H17} cells to expand. Both, 3pRNA and poly(I:C) inhibited the proliferation of CD4⁺ cells, as evidenced by Ki67 staining (Fig. 6d), which was accompanied by a higher percentage of annexin V⁺ apoptotic cells (Fig. 6d). To further elaborate on the survival of antigen-specific T_{H1} and T_{H17} cells, we determined the levels of active caspase-3 protein in splenic T_{H1} or T_{H17} cells derived from EAE mice treated with RLH ligands (Supplementary Fig. 6). We found that both T_{H1} and T_{H17} T cells underwent apoptosis upon ligand challenge, which is consistent with the suppressed T_{H1} and T_{H17} response in the recall assay (Fig. 6a).

We further investigated the proportion of circulating immunosuppressive CD4⁺Foxp3⁺ T_{reg} cells during disease when EAE mice were challenged with dsRNAs (Supplementary Fig. 7). Notably, the percentage of T_{reg} cells did not change after treatment. In addition,

we found no significant changes ($P > 0.05$) in key factors that are important for T_{reg} function (Supplementary Fig. 8).

Given that RNA ligand treatment resulted in a marked reduction of disease severity accompanied by decreased CNS inflammation, we wanted to know whether the treatment effect correlated with a selective reduction of either T_{H1} or T_{H17} CD4⁺ cells in the spleen or CNS of EAE mice (Fig. 6e). Notably, RIG-I and MDA5 activation significantly reduced the numbers of both T_{H1} and T_{H17} cells in the peripheral and central compartment ($P < 0.05$). The absolute numbers of spleen CD4⁺ cells were lower in treated mice, whereas the numbers of CNS-infiltrating cells were decreased on 3pRNA challenge (Fig. 6e). These findings clearly indicate that immunostimulatory dsRNAs are able to inhibit proliferation and induce apoptosis of MOG₃₅₋₅₅-specific T_{H1} and T_{H17} T cells without affecting the ratio and function of CD4⁺Foxp3⁺ T_{reg} cells.

Effect of RLH activation on T_{H17} differentiation

We next assessed the ability of T cells to polarize into effector T cells *in vitro* in the presence of IFN- β , 3pRNA and poly(I:C) (Fig. 7a). The ability of polarized T_{H1} or T_{H17} T cells to produce IL-17 or IFN- γ , respectively, was not influenced by complexed RNA ligands or by recombinant IFN- β . Accordingly, the capacity to upregulate mRNA encoding the transcription factors T-bet, STAT6 and TGF- β was not affected by RIG-I and MDA5 ligands (data not shown), and T_{H1} and T_{H17} cytokines were substantially induced during *in vitro* differentiation (Supplementary Fig. 9).

We then co-cultured supernatant derived from BMDCs, that were previously stimulated with RNA ligands or recombinant IFN- β , with naive sorted CD4⁺ T cells that undergo T-cell polarization *in vitro* (Fig. 7b,c). Under these conditions, supernatant derived from *Ifnar1^{+/+}* BMDCs, but not *Ifnar1^{-/-}* BMDCs, was able to suppress the generation of both IL-17- and IFN- γ -producing CD4⁺ cells.

These data collectively suggest that RNA ligand-mediated disease amelioration is mediated by soluble factors such as type I IFNs or IL-27 derived from RLH-stimulated dendritic cells and that these factors finally inhibit encephalitogenic T_{H1} and T_{H17}

immune responses^{38,39}. However, IL-27-deficient mice showed significant disease amelioration ($P < 0.05$) on ligand treatment (data not shown).

Taken together, our data indicate that T_H17 and T_H1 immune responses during CNS autoimmunity can be suppressed by RNA ligands of the cytosolic receptors RIG-I and MDA5. Subsequent signaling

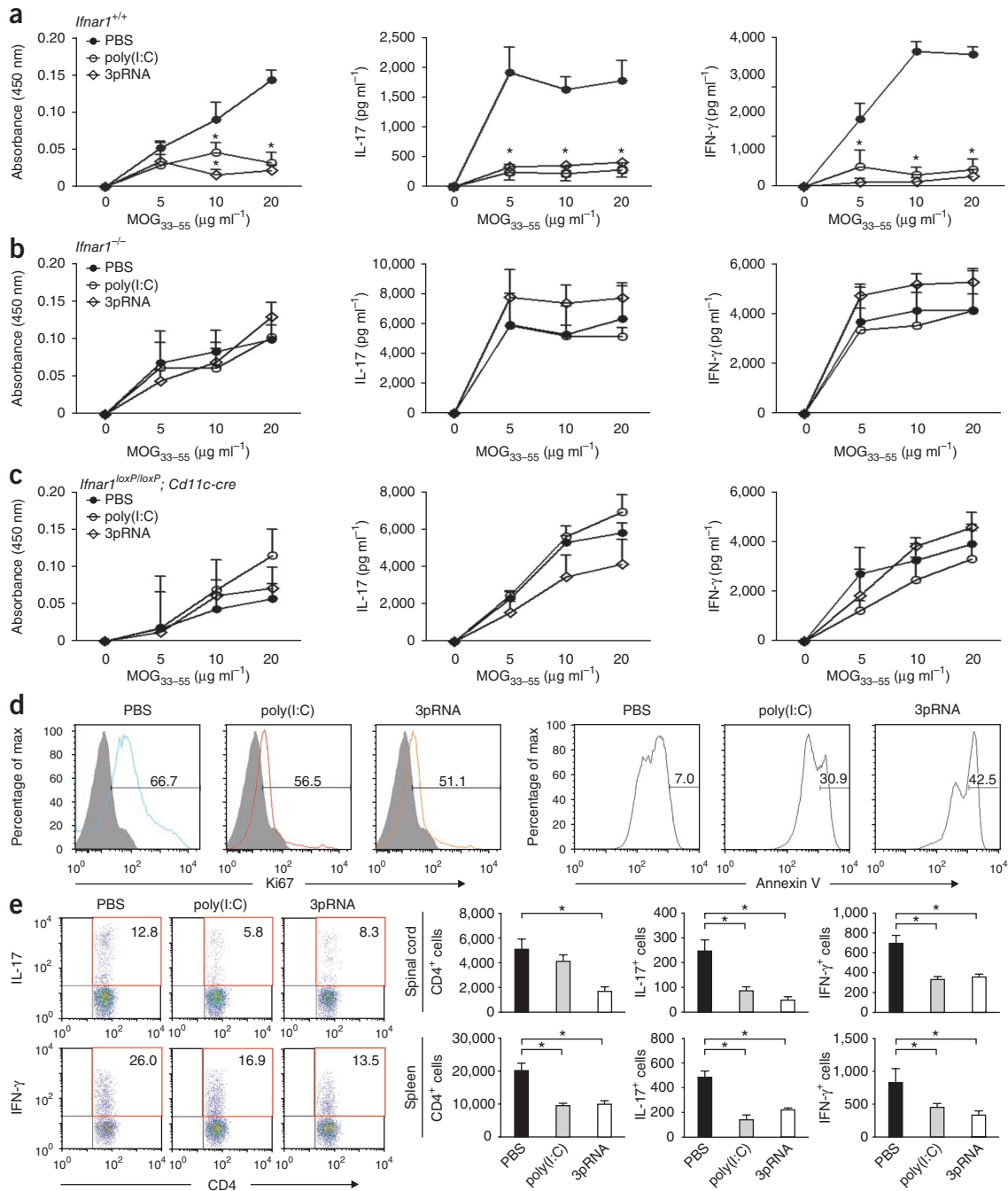


Figure 6 RLH stimulation interferes with T_H1 and T_H17 expansion and survival. **(a–c)** Expansion of antigen-specific T lymphocytes at different MOG_{35–55} concentrations in lymph nodes of *Ifnar1*^{+/+} **(a)**, *Ifnar1*^{-/-} **(b)** and *Ifnar1*^{loxP/loxP}; *Cd11c-cre* **(c)** mice treated with PBS, complexed poly(I:C) and complexed 3pRNA. Lymph nodes were collected at 18 dpi and cultured for 48 h at indicated MOG_{35–55} concentrations. Proliferation was measured by BrdU incorporation for 16 h (left). IL-17 (middle) and IFN-γ (right) release were measured by ELISA. Data represent mean ± s.e.m. One representative experiment out of two is shown. **(d)** RLH treatment inhibited splenocyte proliferation and increased apoptosis. Left, Ki67 flow cytometry analysis of CD4⁺ splenocytes in diseased mice 24 h after a single treatment with PBS, poly(I:C) and 3pRNA. The filled gray area is the isotype control. Right, annexin V staining for apoptotic cells 24 h after ligand challenge. Only CD4⁺ cells were gated and the percentages of Ki67- or annexin V-expressing cells are depicted. Data are representative of two independent experiments. Numbers indicate the percentage of positively labeled cells. **(e)** *Ex vivo* analysis of IL-17 and IFN-γ in spleen and spinal cord of diseased mice after third ligand treatment at 18 dpi and measurement by flow cytometry analysis 24 h later. Events of flow cytometry were gated on CD4⁺ cells. Left, percentages of IL-17- and IFN-γ-producing CD4⁺ T cells in the spleen. Right, quantification of CD4, IL-17 and IFN-γ⁺ cells normalized to 25,000 B220⁺ cells in the spleen or to 25,000 CD45^{lo}CD11b^{hi} microglia in the spinal cord, respectively. Numbers indicate the percentage of each cell population in the quadrant. Quantitative data are expressed as mean ± s.e.m. and summarized from three independent experiments. * $P < 0.05$.

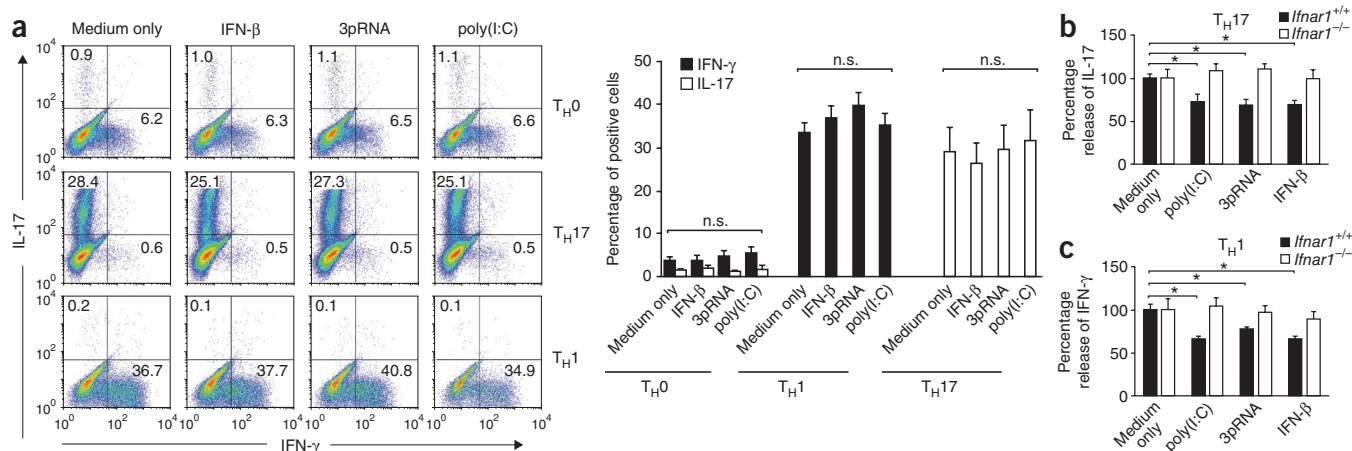


Figure 7 Engagement of RIG-I and MDA5 does not shape normal T-cell differentiation. **(a)** *In vitro* differentiation of naive T cells in the presence of dsRNA. MACS-sorted CD4⁺ T cells were activated with antibodies to CD3 and CD28 and polarized by cytokine treatment to achieve T_{H0}, T_{H17} or T_{H1} differentiation. Numbers indicate the percentage of each cell population in the quadrant. All T-cell subsets were co-incubated for 72 h with medium only, IFN-β (100 U ml⁻¹), complexed 3pRNA (200 ng ml⁻¹) or complexed poly(I:C) (200 ng ml⁻¹). Intracellular cytokines were stained with phycoerythrin-conjugated IL-17 and FITC-conjugated IFN-γ antibodies. The proportions of IL-17⁺ and IFN-γ⁺ cells (left) and quantification (right) are shown. Data represent mean ± s.e.m. One representative experiment out of three is shown. **(b,c)** Differentiation of naive MACS-sorted CD4⁺ T cells activated with antibodies to CD3 and CD28 and polarized for T_{H1} or T_{H17} differentiation for 72 h. T cells were co-cultured for the whole period with conditioned medium from *Ifnar1*^{+/+} or *Ifnar1*^{-/-} BMDCs stimulated before for 24 h either with medium only, lipofectamine-complexed poly(I:C) (200 ng ml⁻¹), lipofectamine-complexed 3pRNA (200 ng ml⁻¹) or IFN-β (100 U ml⁻¹). The amounts of IL-17 **(b)** and IFN-γ **(c)** in the supernatants were measured by ELISA and relative cytokine amounts were compared with the medium controls. Data represent mean ± s.e.m. One representative experiment out of three is shown. **P* < 0.05.

elicits a type-I IFN response that inhibits T-cell expansion and induces T-cell apoptosis via a loop through IFNAR engagement on dendritic cells (**Supplementary Fig. 10**).

DISCUSSION

Here we addressed the role of specific pattern recognition receptors, namely cytosolic helicases such as RIG-I and MDA5 and their adaptor IPS-1, in the formation of pathogenic T_{H1} and T_{H17} cells during autoimmune inflammation of the brain. We demonstrate for the first time, to the best of our knowledge, that the IPS-1 pathway is important for the pathogenesis of CNS autoimmunity, as it limits the propagation of encephalitogenic CD4⁺ T cells. We found that activation of RIG-I and MDA5 by immunostimulatory RNA ligands has a protective role during the effector phase of disease, and reduces CNS pathology and the recruitment of myeloattractants. This beneficial effect was IFNAR dependent and was associated with a suppression of *in vivo* expansion and survival of antigen-specific encephalitogenic and committed IL-17- and IFN-γ-producing CD4⁺ cells.

Several studies have found that TLRs and interferons are important for modulating multiple sclerosis, as well as EAE⁴⁰. Indeed, IFN-β, a type I interferon, is a first line therapy in the treatment of relapsing-remitting multiple sclerosis⁴¹. Notably, exogenously added recombinant IFN-β is effective only in a certain percentage of affected individuals, as up to one third of them develop neutralizing antibodies to IFN-β after 6–18 months of treatment, leading to a loss of drug bioactivity³². This unavoidable situation leads to a reduction in the biological and clinical efficacy of IFN-β. The induction of endogenously produced type I IFN by RIG-I and MDA5 engagement avoids the formation of these antibodies to IFN-β.

An important question is how systemic administration of RNA molecules results in the observed reduction of autoimmune inflammation in the CNS. Because RLHs are expressed in immune cells, receptor engagement of RIG-I and MDA5 leads to direct and indirect activation of immune cell subsets, and we found that immunomodulatory

RNAs induced robust type I IFN production in conventional dendritic cells, plasmacytoid dendritic cells and macrophages.

Intravenous application of RNA complexed with PEI elicited a strong systemic IFN induction as early as 6 h after injection that was paralleled by a rapid clinical improvement after 24–48 h. In principle, several mechanisms of disease protection could be involved, such as inhibition of antigen processing and presentation, suppression of T-cell expansion and maintenance, modulation of cytokine production, and downregulation of matrix metalloproteinases and adhesion molecules, resulting in the inhibition of lymphocyte migration across the blood-brain barrier. A recent study investigated the effect of IFN-β on different subsets of human T cells, namely T_{H0}, T_{H1} and T_{H17} cells⁴². Notably, of the T cell subsets tested, T_{H17} cells were most susceptible to IFN-β-mediated effects, presumably owing to a higher expression of the IFNAR1 chain in T_{H17} cells as compared with T_{H1} lymphocytes. As a possible mechanism, the authors proposed that IFN-β-mediated apoptosis of T_{H17} cells leads to a preferential loss of IL-17-producing cells.

Our results support this possibility, as dsRNA treatment resulted in increased apoptosis and inhibited the proliferation of committed encephalitogenic T cells. Of note, other mononuclear cell populations invading the diseased CNS during EAE, such as Foxp3⁺ T_{reg} cells, CD8⁺ cells, and Ly-6C^{hi} and Ly-6C^{lo} monocytes, were also diminished after treatment, indicating that these cell types might also contribute to disease amelioration. Indeed, the previous study did not rule out the involvement of other cell types such as APCs⁴². This is of particular interest, as several recent reports have suggested that the inhibitory effect of IFN-β is mediated via APCs. Two recent studies investigated the role of IFNAR expression on myeloid cells and observed a more severe EAE with enhanced effector phase and increased lethality in the absence of IFNAR, whereas mice with T or B cell-restricted IFNAR deficiency did not succumb to more severe disease^{30,31}. Notably, one of these studies used *Ifnar1*^{loxP/loxP}; *LysM-cre* mice, in which *Ifnar1* is deleted in specific myeloid subsets³¹. We also

used this strain when we challenged diseased mice with RNA ligands to activate cytoplasmic helicases, but did not observe any ligand-mediated effects when IFNAR was specifically lacking on Ly-6C^{lo} monocytes, Ly-6C^{hi} monocytes, CD11b⁺CD45^{lo} microglia and Gr-1⁺ granulocytes. In contrast, we found that dendritic cells were the main cellular targets when type I IFNs were induced in the periphery.

These data provide evidence that dendritic cells, rather than monocytes and macrophages, are the main immunoregulatory cell type that responds to RLH activation *in vivo*. This selective and nonredundant IFNAR engagement on macrophages versus dendritic cells during CNS autoimmunity may be a result of distinct spatial and temporal effects of type I IFNs produced either locally in the CNS or in secondary lymphoid organs in the periphery. However, we cannot completely rule out the possibility that activated circulating monocytes or microglia upregulating CD11c during inflammation may undergo some Cre expression in *Cd11c-cre* mice.

A recent study found that engagement of IFNAR on dendritic cells inhibits T_H17 priming via osteopontin-dependent production of IL-27 (ref. 43). Another study found that activation of various TLRs provokes IL-27 production by human macrophages, which is mediated by IFN- α -driven transactivation of the p28 subunit of IL-27 (ref. 44). Our data, however, did not support the idea that disease suppression induced by activation of the RIG-I and MDA5 signaling pathways in innate cells is mediated by IL-27.

Under these circumstances and based on the efficacy of RLH ligands in inducing type I interferons that dampen autoimmune inflammation and demyelination in the CNS, it is possible that other effects might also influence disease outcome on helicase activation. Given that recognition of 3pRNA by RIG-I is largely independent of the RNA sequence, anti-T_H17 activities can be elicited by 3pRNA. It is attractive to speculate that short dsRNA molecules can be designed to target mRNA encoding important regulators of T_H1 and T_H17 immune responses, such as T-bet, IL-23p19, IL-17, IL-27 or others. Thus, 3p-short interfering RNAs could be developed that simultaneously silence T_H1- and T_H17-relevant genes and activate RIG-I. This approach could lead to a new class of RNA molecules with dual function for the treatment of autoimmunity.

METHODS

Methods and any associated references are available in the online version of the paper at <http://www.nature.com/natureneuroscience/>.

Note: Supplementary information is available on the Nature Neuroscience website.

ACKNOWLEDGMENTS

We thank A.-K. Gersmann, M. Oberle, D. Kreuz and K. Wolter for excellent technical assistance, A. Diefenbach, H. Jumaa and H. Eibel for scientific advice and S. Brendecke for critical reading. This manuscript is dedicated to Benedikt Volk, former director of the Department of Neuropathology in Freiburg, who devoted his whole life to the exploration of the brain, as an eternal source of inspiration.

This work was supported by KFO177, SFB670 and SFB704 of the German Research Council (DFG), and a Biofuture and a Go-Bio grant of the Bundesministerium für Bildung und Forschung (BMBF) to G.H., a DFG Graduiertenkolleg 1202 fellowship to C.M., the Center of Integrated Protein Science Munich, a research professorship and a "BayImmune" grant to S.E. M.P. was supported by the BMBF-funded Competence Network of Multiple Sclerosis, the Competence Network of Neurodegenerative Disorders, the Center of Chronic Immunodeficiency (CCI), the DFG (SFB 620, FOR1336 and PR 577/8-1) and the Gemeinnützige Hertie-Foundation.

AUTHOR CONTRIBUTIONS

A.D., H.P., A.L.C., S.G., K.K., M.K., D.P., C.M., S.G.M., H.W. and K.-P.K. conducted the experiments. U.K., S.E., S.A. and A.W. contributed to the *in vivo* studies and provided mice or reagents. A.D., H.P., G.H. and M.P. wrote the manuscript. M.P. supervised the project.

COMPETING FINANCIAL INTERESTS

The authors declare no competing financial interests.

Published online at <http://www.nature.com/natureneuroscience/>.

Reprints and permissions information is available online at <http://www.nature.com/reprints/index.html>.

- Steinman, L. A brief history of T_H17, the first major revision in the T_H1/T_H2 hypothesis of T cell-mediated tissue damage. *Nat. Med.* **13**, 139–145 (2007).
- Ivanov, I.I. *et al.* The orphan nuclear receptor ROR γ directs the differentiation program of proinflammatory IL-17⁺ T helper cells. *Cell* **126**, 1121–1133 (2006).
- Komiyama, Y. *et al.* IL-17 plays an important role in the development of experimental autoimmune encephalomyelitis. *J. Immunol.* **177**, 566–573 (2006).
- Hofstetter, H.H. *et al.* Therapeutic efficacy of IL-17 neutralization in murine experimental autoimmune encephalomyelitis. *Cell. Immunol.* **237**, 123–130 (2005).
- Langrish, C.L. *et al.* IL-23 drives a pathogenic T cell population that induces autoimmune inflammation. *J. Exp. Med.* **201**, 233–240 (2005).
- Tzartos, J.S. *et al.* Interleukin-17 production in central nervous system-infiltrating T cells and glial cells is associated with active disease in multiple sclerosis. *Am. J. Pathol.* **172**, 146–155 (2008).
- Bettelli, E. *et al.* Loss of T-bet, but not STAT1, prevents the development of experimental autoimmune encephalomyelitis. *J. Exp. Med.* **200**, 79–87 (2004).
- Stromnes, I.M., Cerretti, L.M., Liggett, D., Harris, R.A. & Goverman, J.M. Differential regulation of central nervous system autoimmunity by T_H1 and T_H17 cells. *Nat. Med.* **14**, 337–342 (2008).
- Kroenke, M.A., Carlson, T.J., Andjelkovic, A.V. & Segal, B.M. IL-12- and IL-23-modulated T cells induce distinct types of EAE based on histology, CNS chemokine profile, and response to cytokine inhibition. *J. Exp. Med.* **205**, 1535–1541 (2008).
- Heppner, F.L. *et al.* Experimental autoimmune encephalomyelitis repressed by microglial paralysis. *Nat. Med.* **11**, 146–152 (2005).
- Fierz, W., Endler, B., Reske, K., Wekerle, H. & Fontana, A. Astrocytes as antigen-presenting cells. I. Induction of Ia antigen expression on astrocytes by T cells via immune interferon and its effect on antigen presentation. *J. Immunol.* **134**, 3785–3793 (1985).
- Kawai, T. & Akira, S. The roles of TLRs, RLRs and NLRs in pathogen recognition. *Int. Immunol.* **21**, 317–337 (2009).
- Matzinger, P. Tolerance, danger, and the extended family. *Annu. Rev. Immunol.* **12**, 991–1045 (1994).
- Akira, S., Uematsu, S. & Takeuchi, O. Pathogen recognition and innate immunity. *Cell* **124**, 783–801 (2006).
- Pichlmair, A. & Reis e Sousa, C. Innate recognition of viruses. *Immunity* **27**, 370–383 (2007).
- Sabbah, A. *et al.* Activation of innate immune antiviral responses by Nod2. *Nat. Immunol.* **10**, 1073–1080 (2009).
- Vilaysane, A. & Muruve, D.A. The innate immune response to DNA. *Semin. Immunol.* **21**, 208–214 (2009).
- Schlee, M. *et al.* Recognition of 5' triphosphate by RIG-I helicase requires short blunt double-stranded RNA as contained in panhandle of negative-strand virus. *Immunity* **31**, 25–34 (2009).
- Hornung, V. *et al.* 5'-triphosphate RNA is the ligand for RIG-I. *Science* **314**, 994–997 (2006).
- Pichlmair, A. *et al.* Activation of MDA5 requires higher order RNA structures generated during virus infection. *J. Virol.* **83**, 10761–10769 (2009).
- Kato, H. *et al.* Differential roles of MDA5 and RIG-I helicases in the recognition of RNA viruses. *Nature* **441**, 101–105 (2006).
- Kawai, T. *et al.* IPS-1, an adaptor triggering RIG-I- and Mda5-mediated type I interferon induction. *Nat. Immunol.* **6**, 981–988 (2005).
- Xu, L.G. *et al.* VISA is an adapter protein required for virus-triggered IFN- β signaling. *Mol. Cell* **19**, 727–740 (2005).
- Meylan, E. *et al.* Cardif is an adaptor protein in the RIG-I antiviral pathway and is targeted by hepatitis C virus. *Nature* **437**, 1167–1172 (2005).
- Seth, R.B., Sun, L., Ea, C.K. & Chen, Z.J. Identification and characterization of MAVS, a mitochondrial antiviral signaling protein that activates NF- κ B and IRF 3. *Cell* **122**, 669–682 (2005).
- Wang, Y. *et al.* *Rig-I*^{-/-} mice develop colitis associated with downregulation of G α i2. *Cell Res.* **17**, 858–868 (2007).
- Smyth, D.J. *et al.* Shared and distinct genetic variants in type 1 diabetes and celiac disease. *N. Engl. J. Med.* **359**, 2767–2777 (2008).
- Nejentsev, S., Walker, N., Riches, D., Egholm, M. & Todd, J.A. Rare variants of IFIH1, a gene implicated in antiviral responses, protect against type 1 diabetes. *Science* **324**, 387–389 (2009).
- Sutton, C.E. *et al.* Interleukin-1 and IL-23 induce innate IL-17 production from gammadelta T cells, amplifying T_H17 responses and autoimmunity. *Immunity* **31**, 331–341 (2009).
- Guo, B., Chang, E.Y. & Cheng, G. The type I IFN induction pathway constrains T_H17-mediated autoimmune inflammation in mice. *J. Clin. Invest.* **118**, 1680–1690 (2008).



31. Prinz, M. *et al.* Distinct and nonredundant *in vivo* functions of IFNAR on myeloid cells limit autoimmunity in the central nervous system. *Immunity* **28**, 675–686 (2008).
32. Mitsdoerffer, M. & Kuchroo, V. New pieces in the puzzle: how does interferon-beta really work in multiple sclerosis? *Ann. Neurol.* **65**, 487–488 (2009).
33. Prinz, M. & Kalinke, U. New lessons about old molecules: how type I interferons shape T_h1/T_h17-mediated autoimmunity in the CNS. *Trends Mol. Med.* **16**, 379–386 (2010).
34. Mildner, A. *et al.* CCR2⁺Ly-6C^{hi} monocytes are crucial for the effector phase of autoimmunity in the central nervous system. *Brain* **132**, 2487–2500 (2009).
35. Prinz, M. & Priller, J. Tickets to the brain: role of CCR2 and CX(3)CR1 in myeloid cell entry in the CNS. *J. Neuroimmunol.* **224**, 80–84 (2010).
36. Prinz, M., Priller, J., Sisodia, S.S. & Ransohoff, R.M. Heterogeneity of CNS myeloid cells and their roles in neurodegeneration. *Nat. Neurosci.* **14**, 1227–1235 (2011).
37. Cucak, H., Yrlid, U., Reizis, B., Kalinke, U. & Johansson-Lindbom, B. Type I interferon signaling in dendritic cells stimulates the development of lymph node-resident T follicular helper cells. *Immunity* **31**, 491–501 (2009).
38. Batten, M. *et al.* Interleukin 27 limits autoimmune encephalomyelitis by suppressing the development of interleukin 17-producing T cells. *Nat. Immunol.* **7**, 929–936 (2006).
39. Stumhofer, J.S. *et al.* Interleukin 27 negatively regulates the development of interleukin 17-producing T helper cells during chronic inflammation of the central nervous system. *Nat. Immunol.* **7**, 937–945 (2006).
40. Prinz, M. *et al.* Innate immunity mediated by TLR9 modulates pathogenicity in an animal model of multiple sclerosis. *J. Clin. Invest.* **116**, 456–464 (2006).
41. Steinman, L., Martin, R., Bernard, C., Conlon, P. & Oksenberg, J.R. Multiple sclerosis: deeper understanding of its pathogenesis reveals new targets for therapy. *Annu. Rev. Neurosci.* **25**, 491–505 (2002).
42. Durelli, L. *et al.* T-helper 17 cells expand in multiple sclerosis and are inhibited by interferon-beta. *Ann. Neurol.* **65**, 499–509 (2009).
43. Shinohara, M.L., Kim, J.H., Garcia, V.A. & Cantor, H. Engagement of the type I interferon receptor on dendritic cells inhibits T helper 17 cell development: role of intracellular osteopontin. *Immunity* **29**, 68–78 (2008).
44. Pirhonen, J., Siren, J., Julkunen, I. & Matikainen, S. IFN-alpha regulates Toll-like receptor-mediated IL-27 gene expression in human macrophages. *J. Leukoc. Biol.* **82**, 1185–1192 (2007).

ONLINE METHODS

Mice. *Ifnar1*^{-/-} mice⁴⁵, originally provided by R.M. Zinkernagel (University of Zurich) were backcrossed to C57BL/6 more than 20 times. Mice carrying *loxP*-flanked *Ifnar1*^{31,46} were crossed with transgenic mice expressing Cre recombinase under the control of either the *LysM*⁴⁷ or *Cd11c* promoters³⁷, each back crossed more than ten times to C57BL/6. *Rig-I*^{-/-}, *Mda5*^{-/-}, *Ips-1*^{-/-} and TLR7-deficient mice were described previously^{21,48,49}.

Induction of EAE and treatment. Female 8–10-week-old mice from each group were immunized subcutaneously with 200 µg of MOG_{35–55} peptide emulsified in complete Freund's adjuvant containing 1 mg of *Mycobacterium tuberculosis* (H37RA, Difco Laboratories). The mice received intraperitoneal injections of 250 ng pertussis toxin (Sigma-Aldrich) at the time of immunization and 48 h later. For treatment studies, mice were injected with 200 µl of PBS containing nucleic acids with prior jetPEI-complexation according to the manufacturer's protocol. In short, 10 µl of *in vivo* jetPEI were mixed with 25 µg of nucleic acids at a N:P ratio of 10:1 in a volume of 200 µl of 5% glucose solution (vol/vol) and incubated for 15 min. Subsequently, 25 µg of complexed or non-complexed 5'-triphosphate RNA or the synthetic dsRNA analog poly(I:C) were injected intravenously at the indicated time points. Whole blood was obtained by retro-orbital puncture at the indicated time points. Serum was prepared from whole blood by centrifugation (13,000 rpm, 5 min). All animal experiments were approved by the ethics review board for animal studies at the Universities of Göttingen and Freiburg.

Clinical evaluation. Mice were scored daily as follows: 0, no detectable signs of EAE; 0.5, distal limp tail; 1.0, complete limp tail; 1.5, limp tail and hindlimb weakness; 2, unilateral partial hindlimb paralysis; 2.5, bilateral partial hindlimb paralysis; 3, complete bilateral hindlimb paralysis; 3.5, complete hindlimb paralysis and unilateral forelimb paralysis; 4, total paralysis of forelimbs and hindlimbs.

Histology. Histology was performed as described recently^{34,40,50}. Spinal cords were removed on day 35 after immunization and fixed in 4% buffered formalin (vol/vol). Spinal cords were then dissected and embedded in paraffin before staining with hemalaun and eosin, LFB to assess the degree of demyelination, MAC-3 (BD Pharmingen) for macrophages and microglia, CD3 for T cells, APP to determine axonal damage, and NOGO-A for mature oligodendrocytes (Serotec). Spinal cord sections were evaluated using the cell-P software (Olympus).

Flow cytometry. Cells were stained with primary antibodies to CD3, CD8, Ly-6C, Ly-6G, CD115, CD25, CD11b, CD11c, CD4 and CD45 (BD Bioscience) for 30 min at 4 °C. For intracellular staining of IL-17 and IFN-γ, cells were activated with ionomycin (1 µg ml⁻¹), phorbol myristate acetate (50 ng ml⁻¹) and Golgipost (BD Bioscience) for 4 h. Intracellular staining of IL-17, IFN-γ, Ki67, activated caspase 3 and Foxp3 was performed with the corresponding staining kits (BD Bioscience and eBioscience) according to the manufacturer's protocol. Annexin V (BD Bioscience) staining was performed after surface staining with antibodies to CD4 according to manufacturer's instructions.

For flow cytometry of spinal cord and spleen, mice were immunized and treated with RLH ligands or PBS at 13, 15 and 17 dpi. Mice were subsequently perfused with cold PBS and tissue was taken. Spinal cords were then treated with collagenase and dispase (2 mg ml⁻¹, Roche) for 30 min and strained through nylon meshes. Cells were isolated by density gradient centrifugation (Percoll, Sigma-Aldrich). Cells were washed and analyzed using a FACSCanto (Becton Dickinson). Viable cells were gated by forward and side scatter pattern. Data were acquired with FACSdiva software (Becton Dickinson). Post-acquisition analysis was performed using FlowJo software (Tree Star).

Recall assay. Mice were injected three times intravenously with PBS, complexed poly(I:C) (25 µg) or complexed 3pRNA (25 µg) at 13, 15 and 17 dpi. On day 18, the draining axillary and inguinal lymph nodes were removed and single cell suspensions were prepared. We placed 6 × 10⁵ lymph node cells as triplicates in a 96-well plate and pulsed them with the indicated dosages of MOG_{35–55} peptide. BrdU uptake was measured for 16 h to determine proliferation (Cell Proliferation ELISA colorimetric, Roche Applied Science) according to the manufacturer's protocol. For cytokine analysis, sister cultures supernatants were analyzed by ELISA for IFN-γ and IL-17 (R&D Systems).

T-cell differentiation. For the differentiation of naive T cells, spleen and lymph nodes of C57BL/6 mice were strained through a 40-µm mesh. Isolation was performed using the magnetic cell separation system (MACS) for CD4⁺ selection (Miltenyi Biotec) according to the manufacturer's protocol. We cultured 2 × 10⁵ CD4⁺ cells in RPMI1640 containing 10% fetal calf serum (vol/vol, Gibco), 100 U ml⁻¹ penicillin and 100 µg ml⁻¹ streptomycin (Invitrogen). T cells were subsequently activated with soluble antibodies to CD3 (4 µg ml⁻¹) and CD28 (30 ng ml⁻¹) and polarized in the presence of cytokines for 120 h to achieve either T_H0 (no additional cytokines), T_H1 (6 ng ml⁻¹ rIL-12) or T_H17 (20 ng ml⁻¹ rIL-6, 5 ng ml⁻¹ rhTGF-β, 10 ng ml⁻¹ rIL23 and 10 µg ml⁻¹ antibody to IFN-γ) cells. All cytokines were purchased from R&D Systems.

For co-incubation experiments, triplicates of each T-cell subset were stimulated with either medium, 100 U ml⁻¹ IFN-β, 200 ng ml⁻¹ lipofectamine-transfected poly(I:C) or 200 ng ml⁻¹ lipofectamine-transfected 5'-triphosphate RNA starting at the beginning of differentiation. Replacement of media was performed after 48 h. Flow cytometric analysis for IFN-γ and IL-17 was carried out after 120 h.

For naive T-cell differentiation with BMDC-derived supernatant, 10⁵ BMDCs per well were treated with indicated ligands 24 h before T-cell differentiation. T cells were then polarized with T_H0-, T_H1- or T_H17-inducing conditions (ratio of supernatant to cytokine cocktail was 1:1).

Detection of injected RNA *ex vivo* using flow cytometry analysis. Diseased mice were injected intravenously with FITC-labeled RNA (25 µg) complexed with jetPEI (25 µg) or PBS as a control. After 12 h, spleens and spinal cords were taken and single cell suspensions were prepared. Cells were surface stained with antibodies to CD4, CD11b and CD11c, and FITC-labeled RNA uptake was analyzed by flow cytometry.

Real-time PCR. Tissue was dissected and flushed with ice-cold Hanks balanced salt solution. RNA was isolated using the RNeasy Mini Kit (Qiagen) following the manufacturer's instructions. Samples were treated with DNaseI (Roche) and 1 µg of RNA was transcribed into cDNA using oligo-dT primers and the SuperScript II RT kit (Invitrogen). 2.5 µl cDNA were transferred into a 96-well Multiply PCR plate (Sarstedt) and 12.5 µl Absolute QPCR SYBR Green master mix (Thermo Fisher) plus 19.6 µl ddH₂O were added. RT-PCR reactions were performed as described recently⁴⁰.

Media and reagents. RPMI 1640 (Invitrogen) and Dulbecco's modified Eagle's medium (Invitrogen) each supplemented with 10% fetal calf serum, 3 mM L-glutamine, 100 U ml⁻¹ penicillin and 100 µg ml⁻¹ streptomycin (all from Sigma-Aldrich) were used. Poly(I:C) was obtained from Invivogen. Chemically synthesized RNA oligonucleotides were purchased at MWG-BIOTECH AG. Double-stranded *in vitro* transcribed 3pRNA was generated as described previously²⁹. Synthetic RNA (PolyA5'→3' AAAAAAAAAAAAAAAAAAAAAA or synRNA sense strand 5'→3' GCAUGCGACCUCUGUUUGA; Fig. 4) and 3pRNA (sense strand 5'→3' GCAUGCGACCUCUGUUUGAC) were used in most experiments.

Cells and cytokine measurements. BMDCs and BMDMs were generated and grown as described previously²⁹. *In vitro* experiments with cells including T cells, dendritic cells, splenocytes were stimulated with 200 ng ml⁻¹ 3pRNA or poly(I:C) transfected with Lipofectamine 2000 (Invitrogen) for 24 h, respectively. Transfection was performed according to the manufacturer's instructions. For some experiments, cells were isolated from spleens or lymph nodes of wild-type mice by MACS using the mouse B cell isolation kit and CD19 microbeads or the CD4⁺ selection kit (Miltenyi Biotec) for T cells. Untouched NK cells and CD8 T cells were sorted from spleens using the NK cell isolation and the CD8 T cell isolation kit (Miltenyi Biotec). The viability of all cells was above 95%, as determined by trypan blue exclusion, and purity was >90%, as analyzed by FACS. Cell supernatants and sera were analyzed for cytokine secretion by ELISA for IFN-β, IL-17 and IFN-γ (R&D Systems or PBL Biomedical Laboratories).

Statistical analysis. Statistical differences of clinical scores were evaluated using a nonpaired Student's *t* test. Differences were considered to be significant when *P* < 0.05.

45. Müller, U. *et al.* Functional role of type I and type II interferons in antiviral defense. *Science* **264**, 1918–1921 (1994).
46. Kamphuis, E., Junt, T., Waibler, Z., Forster, R. & Kalinke, U. Type I interferons directly regulate lymphocyte recirculation and cause transient blood lymphopenia. *Blood* **108**, 3253–3261 (2006).
47. Clausen, B.E., Burkhardt, C., Reith, W., Renkawitz, R. & Forster, I. Conditional gene targeting in macrophages and granulocytes using LysMcre mice. *Transgenic Res.* **8**, 265–277 (1999).
48. Heil, F. *et al.* The Toll-like receptor 7 (TLR7)-specific stimulus loxoribine uncovers a strong relationship within the TLR7, 8 and 9 subfamily. *Eur. J. Immunol.* **33**, 2987–2997 (2003).
49. Kumar, H. *et al.* Essential role of IPS-1 in innate immune responses against RNA viruses. *J. Exp. Med.* **203**, 1795–1803 (2006).
50. van Loo, G. *et al.* Inhibition of transcription factor NF- κ B in the central nervous system ameliorates autoimmune encephalomyelitis in mice. *Nat. Immunol.* **7**, 954–961 (2006).

